

Simultaneous removal of potent cyanotoxins from water using magnetophoretic nanoparticle of polypyrrole: adsorption kinetic and isotherm study

S. Hena¹ · R. Rozi¹ · S. Tabassum² · A. Huda¹

Received: 23 August 2015 / Accepted: 21 March 2016 / Published online: 12 April 2016
© Springer-Verlag Berlin Heidelberg 2016

Abstract Cyanotoxins, microcystins and cylindrospermopsin, are potent toxins produced by cyanobacteria in potable water supplies. This study investigated the removal of cyanotoxins from aqueous media by magnetophoretic nanoparticle of polypyrrole adsorbent. The adsorption process was pH dependent with maximum adsorption occurring at pH 7 for microcystin-LA, LR, and YR and at pH 9 for microcystin-RR and cylindrospermopsin (CYN). Kinetic studies and adsorption isotherms reflected better fit for pseudo-second-order rate and Langmuir isotherm model, respectively. Thermodynamic calculations showed that the cyanotoxin adsorption process is endothermic and spontaneous in nature. The regenerated adsorbent can be successfully reused without appreciable loss of its original capacity.

Keywords Adsorption · Conducting polymer · Cylindrospermopsin · Microcystins · PPy/Fe₃O₄

Responsible editor: Philippe Garrigues

Electronic supplementary material The online version of this article (doi:10.1007/s11356-016-6540-5) contains supplementary material, which is available to authorized users.

✉ S. Hena
sufiahena@usm.my

¹ School of Industrial Technology, University Sains Malaysia, George Town, Penang 11800, Malaysia

² School of Environmental Science and Engineering, Shanghai Jiao Tong University, Shanghai 200240, China

Introduction

Numbers of freshwater cyanobacteria produce potent hepatotoxins which lead to serious health risk with acute symptoms of vomiting, diarrhea, and even death (Falconer 2005). The cyanotoxin removals are important to water industries as these are hepatotoxins and promote liver tumor (Falconer 1989). Among all the cyanotoxins, microcystins (MCs) and cylindrospermopsin (CYN) are the most common hepatotoxins recorded in drinking waters produced by *Microcystis aeruginosa* and *Cylindrospermopsis raciborskii* mainly in tropical and sub-tropical regions (Ho et al. 2011). Cyanotoxins are problematic since these are highly soluble and chemically stable in water (Jones and Orr 1994; Wang et al. 2007). Moreover, the dissolved cyanotoxins have been reported to be more recalcitrant towards the conventional methods of water treatment such as, sedimentation, filtration, and coagulation-flocculation (Dixon et al. 2010; Dixon et al. 2011). However, adsorption granular and powdered activated carbons have shown to be successful in removal of cyanotoxins from drinking water (Ho et al. 2011; Hena et al. 2014).

The climate change experts have predicted increase in both the occupied water bodies and intensity of cyanobacterial blooms (Pearl and Huisman 2008); thus, it is an important topic of concern to find out better options to remove cyanotoxins together. To date, many studies have been done for the removal of microcystins (El-Sheikh et al. 2014; Wang et al. 2014; Zhang et al. 2014) and cylindrospermopsin (Fotiou et al. 2015; He et al. 2014) with different methods. Among all the reported methods, adsorption is technically easy and one of the most economically favorable method, although there are very few studies that have been conducted on removal of microcystins and cylindrospermopsin together

(Ho et al. 2011). However, no studies have been yet performed involving conductive electroactive polymer as an adsorbent for removing cyanotoxins from drinking waters.

The main aim of this study was to investigate the adsorption of cyanotoxins on Fe_3O_4 coated with electroactive conducting polymer (ECP) polypyrrole (PPy/ Fe_3O_4) without compromising the quality of drinking water. Polypyrrole (PPy) has been a subject of intense investigation of many research groups because of their interesting qualities such as high electrical conductivity, environmental stability, and non-toxicity, which advocate it to categorize under reusable and environmental friendly material. Its easy and relatively low cost of preparations competes over activated carbon (Bhaumik et al. 2011a; Ansari et al. 2009). PPy matrix carries positive charges due to positive nitrogen atoms which happen to be produce during polymerization reaction. The matrix maintains their neutrality via incorporating the counter ions commonly known as dopant during the course of polymerization reaction (Zhang and Bai 2003). The presence of positively charged nitrogen atoms are being used to form electrostatic bond between any other negatively charged carrying compounds. Previously, PPy have been used for removal of fluoride (Bhaumik et al. 2011b), chromium (IV) (Bhaumik et al. 2011a; Ansari and Fahim 2007), and arsenic (Eisazadeh 2008) from aqueous medium and have proven advantageous adsorbent.

The main objectives of this study were to evaluate an efficient separation method for removing the cyanotoxins from water by PPy/ Fe_3O_4 nanoparticles. The operational parameters in this adsorption process such as temperature effect, initial concentration of adsorbates, time of contact of adsorbate and adsorbent, and solution pH were characterized, and the adsorption mechanism of PPy/ Fe_3O_4 nanoparticles was investigated.

Methods

Materials

Fe_3O_4 , pyrrole (Py), and FeCl_3 were used from Sigma–Aldrich, Germany. The MC-LR, RR, YA, LA, and CYN were supplied by Fluka, Switzerland, and were used without further purification. Hydrochloric acid and sodium hydroxide were used to alter the pH of the solutions as per requirement. All aqueous solutions were prepared using organic molecule free Milli-Q water (18-M Ω resistance).

Synthesis of the magnetic PPy/ Fe_3O_4 nanoparticle

The PPy/ Fe_3O_4 nanoparticles were synthesized by chemical oxidative polymerization of freshly distilled pyrrole monomer

in the presence of FeCl_3 used as an oxidant, as shown in Scheme 1, where $y = n \times m$.

For polymerization of Py, 0.1 g of Fe_3O_4 was added into 30-mL deionized water in a beaker and ultrasonicated for 10 min to dispersed nanoparticles of Fe_3O_4 homogenously into double-distilled deionized water to achieved constant size of PPy/ Fe_3O_4 . A 3 g of oxidant, FeCl_3 , was supplemented into the deionized water having dispersed Fe_3O_4 and was agitated for 10 min on shaker and followed by addition of 0.5 mL of freshly distilled Py. The beaker was kept under continuous shaking for 2.5 h at 23 ± 2 °C ambient room temperature. Finally, after 2.5 h, into the reaction mixture, the acetone was added to stop the polymerization reaction. A black color powdered product was acquired by filtration process and washed with deionized distilled water till the filtrate turn out to be colorless and finally washed twice with analytical grade acetone. The obtained PPy/ Fe_3O_4 nanoparticles were vacuumed dried at 80 °C for 5 h, and analyzed its weight gravimetrically, which was found as 0.51 g. The weight ratio of Fe_3O_4 and PPy was obtained as 1:4. The magnetic property of the PPy/ Fe_3O_4 nanoparticle was analyzed before the recovery of cyanotoxins and after the recovery of PPy/ Fe_3O_4 from cyanotoxins using vibrating sample magnetometer (VSM).

The Brunauer, Emmett, and Teller (BET) surface area of the PPy/ Fe_3O_4 nanoparticle was determined by the low-temperature N_2 adsorption–desorption technique using Micrometrics. SEM analysis of PPy/ Fe_3O_4 nanoparticles was carried out on a field emission JEOL-6500 F scanning electron microscope at 200 kV. The structure of PPy/ Fe_3O_4 nanoparticle was characterized using a JEOL-2010 transmission electron microscope (TEM) at 200 kV. The X-ray photoelectron spectroscopy (XPS) measurement was taken on a Kratos Axis Ultra DLD with monochromatic Al K α X-ray source (1486.6 eV of photons) to determine the N atoms present in the PPy coating and their oxidation states.

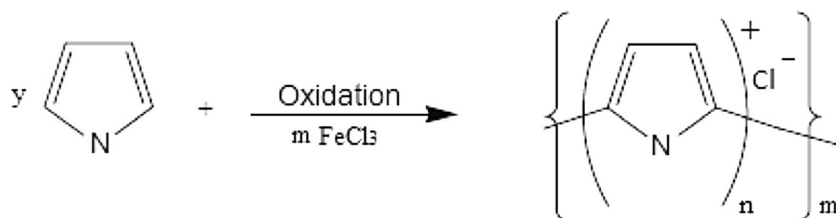
Zeta potential

The zeta (ζ) potential of PPy/ Fe_3O_4 nanoparticle was analyzed by Zeta Potential Analyzer (Beckman Coulter Inc.) at 25 °C. All samples were measured three times, and presented results are mean values.

Batch adsorption studies

Batch studies were carried out at 200 rpm on temperature-controlled shaker with a fixed adsorbent dosage of 10 mg/L using 100 mL of cyanotoxin solution. MCs and CYN were analyzed at different time intervals (0–30 min). Isotherm studies were conducted at different initial concentrations of cyanotoxins (50–200 $\mu\text{g/L}$) in a series of 100-mL Erlenmeyer flasks, and the pH of the water were adjusted at pH 7.0 (for MC-LR, YR, and LA) and pH 9.0 (for CYN and

Scheme 1 Polymerization reaction of polypyrrole



MC-RR). The studies of cyanotoxin adsorption onto PPy/Fe₃O₄ were carried out in the temperature range of 303–323 K to determine the equilibrium adsorption isotherms of each targeted cyanotoxins separately. The equilibrium adsorption capacities were calculated using Eq. (1) as shown below

$$q_e = (C_0 - C_e) \frac{V}{M} \quad (1)$$

where q_e ($\mu\text{g}/\text{mg}$) was the equilibrium adsorption capacity. C_0 and C_e were the initial and equilibrium concentrations ($\mu\text{g}/\text{L}$) of cyanotoxins in their respective solution. V (L) was the volume and M (mg) was the weight of adsorbent.

Desorption studies

The PPy/Fe₃O₄ nanoparticles were regenerated by treating exhausted adsorbent with 2 M HCl or NaOH ranging from pH 1 to 12 for 20 min. After recovery, the abilities of the regenerated PPy/Fe₃O₄ nanoparticles were re-tested for cyanotoxin removal using similar procedure as described in “Batch adsorption studies” section.

Results and discussions

Characteristics of the PPy/Fe₃O₄ nanoparticle

In the present study, the sizes of the spherical particles of Fe₃O₄ and PPy/Fe₃O₄ nanoparticles were reported as 10 and 50–100 nm, respectively. The TEM images (Supplementary Fig. 1a) of two different magnifications suggest that the precipitating PPy moieties encapsulate the suspended Fe₃O₄ nanoparticles, where Fe₃O₄ nanoparticles were used as scaffold for PPy layers (Bhaumik et al. 2011b). The dark central core and light-colored outer layer were due to the different electron penetrabilities (Supplementary Fig. 1b) in Fe₃O₄ and PPy layers, respectively. These features indicate that the nanodimensional Fe₃O₄ particles were embedded in the PPy matrix, forming a core–shell magnetic structure. The SEM image (Supplementary Fig. 1c) reveals the spherical shape of PPy/Fe₃O₄ nanoparticle. The BET surface area of the PPy/Fe₃O₄ magnetic nanoparticle was determined as 13, 169.27 m²/g using low-temperature N₂ adsorption–desorption method.

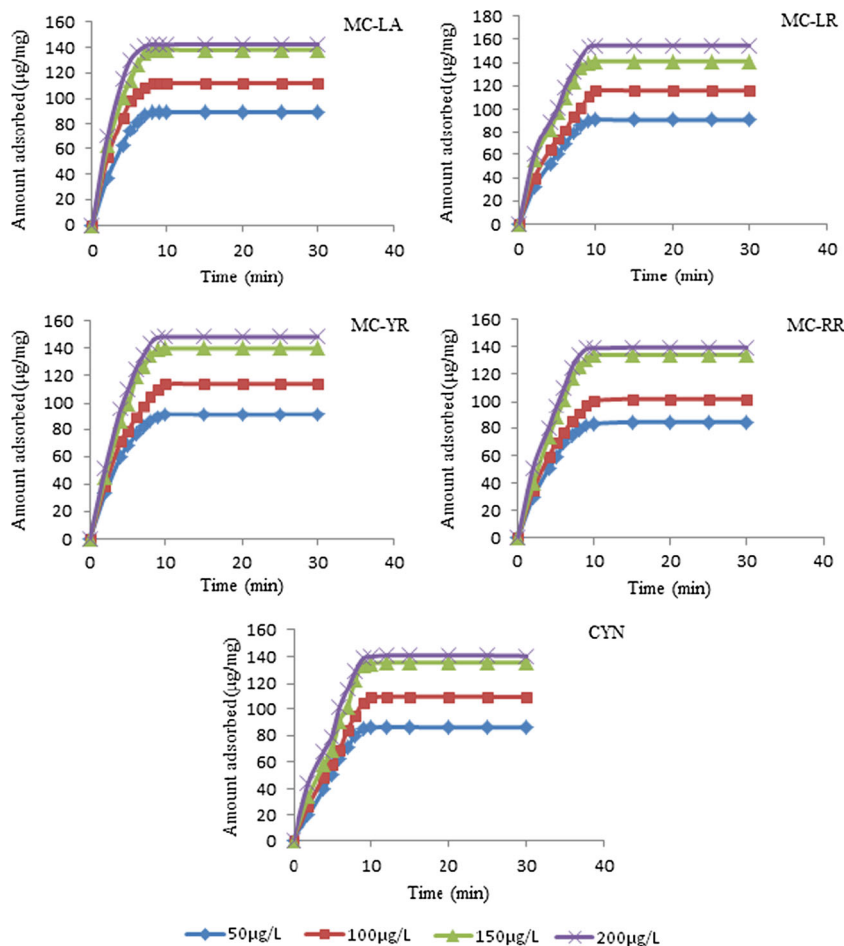
The magnetic property of the PPy/Fe₃O₄ particle was explored using vibrating sample magnetometer at the temperature of 300 K (Supplementary Fig. 2a). The magnetic hysteresis loops (magnetization (M) versus applied field (H) curves) was obtained with the saturation magnetization (M_s) value 70 emu g⁻¹; however, the value was slightly smaller than that of bulk magnetite (Fe₃O₄; 82 emu g⁻¹) discussed by Dunlop and Ozdemir (1997). The value of M_s and exhibiting hysteresis loop while subjected to cyclic magnetic field confirmed the ferrimagnetism behavior of PPy/Fe₃O₄. Supplementary Fig. 2b confirmed that the values of saturation magnetization (M_s), magnetic remanence (M_r), and coercivity (H_c) of the recovered PPy/Fe₃O₄ nanoparticles do not change (Supplementary Fig. 2c), indicating the persisted magnetic property of the PPy/Fe₃O₄ nanoparticles even after the adsorption-desorption process of cyanotoxins from water.

With reference of XPS spectrum in Supplementary Fig. 3, it was observed that 39.5 % of positively charged nitrogen atoms (N⁺) contributed the polypyrrole structure while rest of the nitrogen was amine (–NH–); however, no signal for imine was observed.

Effect of initial concentration of adsorbates and contact time

The trends of adsorption of cyanotoxins onto PPy/Fe₃O₄ nanoparticles with different initial concentration (50–200 $\mu\text{g}/\text{L}$) are shown in Fig. 1. The adsorption of all cyanotoxins onto PPy/Fe₃O₄ nanoparticles increased with time and quickly attained equilibrium state in between 8 and 15 min. The rate of equilibrium attained was found in order of MC-LA < LR = YR < CYN < RR with respect of time, where MC-LA attained its equilibrium at 8 min while MC-RR attained at 15 min. Figure 1 also reveals that the amount of cyanotoxin adsorption also depends upon the concentration of adsorbates present initially in water samples, which increased with increase of initial adsorbate concentration. Additionally, the time curves show that the removals of cyanotoxins are quite rapid till 5 and 6 min but slowly lower down till acquire the equilibrium. At low concentrations of the adsorbates, the ratios of the adsorption sites to the initial toxins are adequate which is concluded as high removal efficiency of adsorbent. Nevertheless, at higher concentrations, the available surface area becomes less compare to the moles of adsorbates present (Sathishkumar et al. 2008; Hena 2010); consequently, the

Fig. 1 Effect of initial concentration of cyanotoxins and contact time



amount adsorb increases with increase in initial concentration from 50 to 200 mg/L, with final different values of toxin removal in different time periods, whereas the removal efficiency decreases as mentioned in Table 1. The removal efficiencies were calculated by using Eq. (2) as below, where C_i and C_e were the initial and equilibrium concentrations of adsorbates ($\mu\text{g}/\text{mg}$), respectively, in the solution.

$$\% \text{ removal efficiency} = \frac{C_i - C_e}{C_i} \times 100 \quad (2)$$

Zeta (ζ) potential of PPy/ Fe_3O_4 and effect of pH

The pH changes the surface properties of the adsorbent as well as the ionic forms of cyanotoxins, and thus, it influences the adsorption capacity of PPy/ Fe_3O_4 nanoparticles. The ionic forms of cyanotoxins at pH 7 are list down in Table 2. In order to further understand the impact of pH on PPy/ Fe_3O_4 nanoparticles and its interactions with cyanotoxins, zeta potential measurements of the PPy/ Fe_3O_4 nanoparticles were carried out (Fig. 2). The zeta potentials of the PPy/ Fe_3O_4 nanoparticles maintain predominantly positive charge over a wide pH range (2–10) with an isoelectric point at pH 10.4 (Fig. 2).

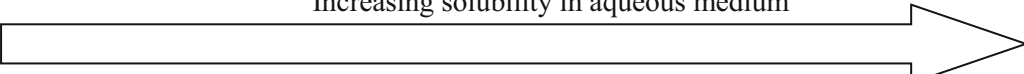
Maximum adsorptions of MC-YR, LR, and LA were found to occur at pH 7, since they are essentially in anionic form above pH 6, and thus, these cyanotoxins can be removed from the drinking water without compromising the quality of water. However, the adsorption decreases at higher pH 9–11, due to the presence of excess OH^- ions competing with MC-YR, LR, and LA, while at lower than pH 4, they possess cationic form which does not favor the adsorption onto positively charged PPy matrix due to electrostatic repulsion.

The maximum adsorptions for MC-RR and CYN were found to occur at pH 9, as shown in Fig. 3. The 99.9 % removal of MC-RR and CYN costs a little compromise in

Table 1 Effect of initial concentrations of adsorbates on removal efficiency of PPy/ Fe_3O_4

| Concentration ($\mu\text{g}/\text{mg}$) | Removal efficiency (%) | | | | |
|---|------------------------|-------|-------|-------|------|
| | MC-LA | MC-LR | MC-YR | MC-RR | CYN |
| 50 | 99.1 | 99.8 | 99.6 | 86.2 | 89.3 |
| 100 | 97.5 | 98.1 | 97.8 | 83.9 | 88.1 |
| 150 | 94.7 | 96.3 | 95.7 | 81.1 | 85.7 |
| 200 | 91.4 | 93.6 | 92.9 | 77.8 | 81.5 |

Table 2 Properties of the cyanotoxins used in present study

| Properties | MC-LA | MC-LR | MC-YR | MCRR | CYN |
|-----------------------------------|--|------------------|-------------------|-------------------|--------|
| Molecular weight (g/mol) | 910.06 | 995.17 | 1045.19 | 1038.20 | 415.43 |
| Variable amino acids | Leucine/Alanine | Leucine/Arginine | Tyrosine/Arginine | Arginine/Arginine | -- |
| Net charge at pH 7 | -2 | -1 | -1 | 0 | 0 |
| Toxicity (LD ₅₀ µg/kg) | 50 | 50 | 70 | 600 | 2100 |
| Solubility in water | Increasing solubility in aqueous medium  | | | | |

quality of drinking water, since the pH of the water become slightly alkaline. However at pH 7, more than 85 % of both MC-RR and CYN were removed. At higher pH 10.4 and above, lower adsorptions of MC-RR and CYN had happen due to the presence of excess OH⁻ ions competing with MC-RR and CYN, while at low pH 2–6, the reason for lower adsorption is same as stated above.

Effect of temperature

The effects of temperature on removal of cyanotoxins with the initial concentration of 50 µg/L using PPy/Fe₃O₄ were studied. The adsorption capacity of cyanotoxin MC-LA, LR, and YR onto PPy matrix increased with rise in temperature of the system from 293 to 323 K at pH 7. Generally, adsorption is an exothermic process because the adsorption of a relatively hydrophobic MC-LA, LR, and YR by a hydrophobic adsorbent PPy/Fe₃O₄ nanoparticle from an aqueous solution should be exothermic, but in present study, it is observed that the adsorption process is endothermic in nature. The enhancement in the

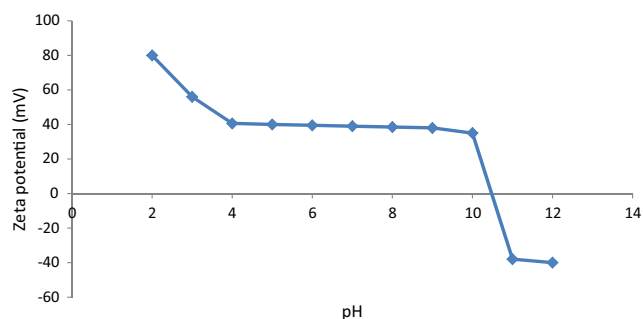
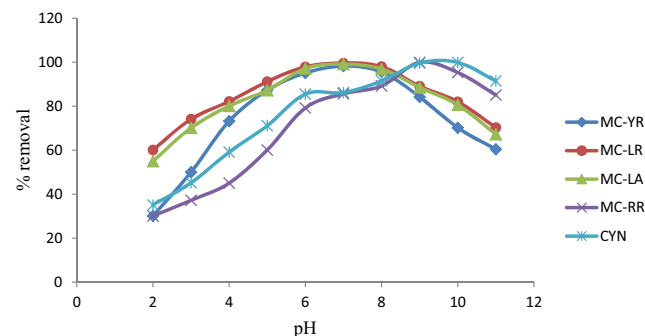
adsorption capacity with increase of temperature may be due to the heat liberated during adsorption of cyanotoxins that were insufficient to compensate for the heat required to displace the solvent (aqueous) (Pendleton et al. 2001). For the adsorption of cyanotoxins at initial concentration of 50 µg/L, the thermodynamic parameters such as changes in entropy (ΔS°), enthalpy (ΔH°), and standard Gibbs free energy (ΔG°) were determined under the influence of temperature range of 293–323 K by using Eqs. (3) and (4), at pH 7 for MC-LA, LR, and YR and pH 9 for MC-RR and CYN by the PPy/Fe₃O₄ (Fig. 4).

$$\Delta G^\circ = -RT \ln K_C \quad (3)$$

where R is the universal gas constant (8.314 J mol⁻¹ K⁻¹), T is the absolute temperature, and K_C is the equilibrium constant.

$$\ln K_C = \Delta S^\circ / R - \Delta H^\circ / RT \quad (4)$$

ΔS° and ΔH° were calculated from the intercept and slope of the graph plotted $\ln K_C$ versus $1/T$ as shown in Fig. 5. The adsorption processes were found endothermic in nature for all

**Fig. 2** Zeta-potentials of PPy/Fe₃O₄ nanoparticles as a function of pH**Fig. 3** Effect of pH on percent removal of cyanotoxins from water

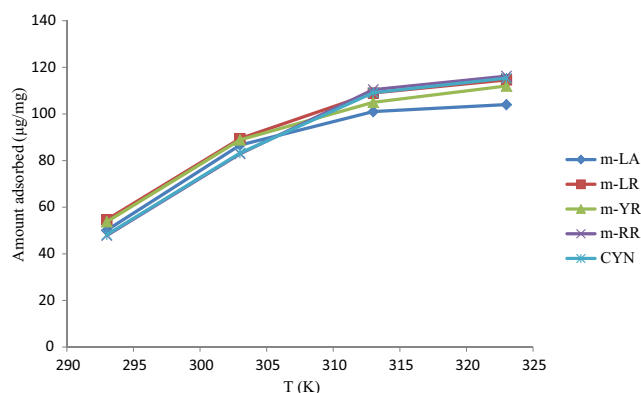
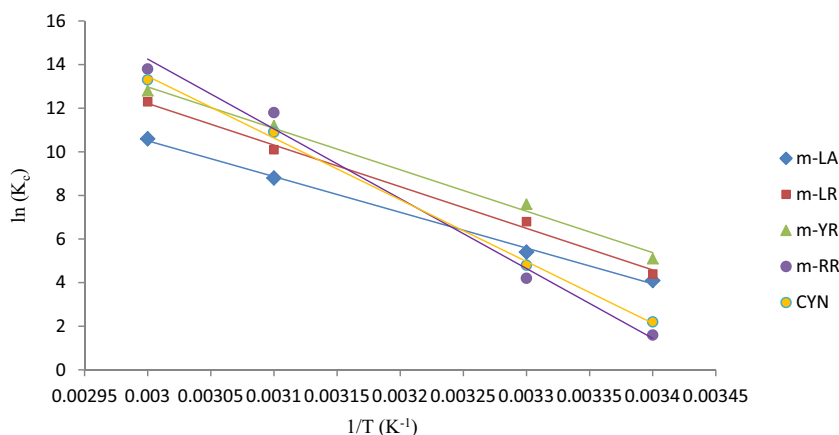


Fig. 4 Effect of temperature on adsorption of cyanotoxins at pH 7 for MC-LA, LR, and YR and at pH 9 for MC-RR and CYN

the cyanotoxins since the ΔH° possessed positive values, while ΔG° increased in its negative magnitude with increase in temperature for every cyanotoxins. The negative magnitudes of ΔG° revealed the viability and spontaneous nature of the adsorption process (Table 3), while higher values of $\ln K_C$ refer as adsorption affinity; the affinities were in the sequence of MC-RR > CYN > MC-YR > MC-LR > MC-LA at 323 K.

The adsorption capacity of cyanotoxin mixture (CTM) onto PPy matrix also reflected the same trend, and it increased with rise in temperature of the system from 293 to 323 K for the initial concentration of total 50 µg/L (mixture of 10 µg/L each of MC-LA, LR, YR, RR, and CYN) at pH 7. The most remarkable finding was that at 323 K, the percent removal of MC-RR and CYN significantly increased from 85.63 and 86.21 % to 92.12 and 94.89 % (Fig. 6), respectively, at pH 7. The adsorption capacity of MC-RR and CYN increased with temperature due to containing less hydrophobicity than others, which might need extra heat energy to displace aqueous molecules. The cyanotoxin removals at pH 8 and 9 for 323 K were analyzed, and removals were found as high as 99 %, since the main aim of this study was simultaneous removal of cyanotoxins at neutral pH from drinking water; thus, the data have not mentioned here for comparisons.

Fig. 5 Plot of $\ln K_C$ versus $1/T$ for adsorption of cyanotoxins onto PPy/Fe₃O₄



Adsorption kinetics

The adsorption kinetic explains the rate of adsorption of uptake of cyanotoxins onto the PPy matrix which controls the equilibrium time. In order to determine the adsorption kinetics of cyanotoxins, the pseudo-first-order and pseudo-second-order models were analyzed to fit the kinetic data.

Pseudo-first-order model

The pseudo-first-order rate model of Lagergren (1898) is based on solid capacity and as described by Eq. (5).

$$\log (q_e - q_t) = \log q_e - k_1 t / 2.303 \quad (5)$$

where k_1 (min^{-1}) is the first-order rate constant, q_t ($\mu\text{g}/\text{mg}$) represents residual concentration of solute at time t in solution, and q_e ($\mu\text{g}/\text{mg}$) is the equilibrium concentration of cyanotoxins present in solutions. In Table 4, the low values of correlation coefficient R^2 show that the adsorption of none of the studied cyanotoxins onto PPy/Fe₃O₄ follows first-order kinetics.

Pseudo-second-order model

The kinetic data were further analyzed using the pseudo-second-order model, which can be expressed as Eq. (6)

$$t/q_t = 1/k_2 q_e^2 + t/q_e \quad (6)$$

where k_2 ($\text{mg}/\mu\text{g min}$) is the second-order rate constant and q_t is the amount adsorbed at time t . From Table 4, the values ($R^2 \approx 0.989\text{--}0.998$) of the correlation coefficients R^2 of the pseudo-second-order model gave better description of the cyanotoxin adsorption compared to pseudo-first-order model ($R^2 \approx 0.802\text{--}0.942$).

The pseudo-second-order model has been successfully applied to the adsorption of pollutants from aqueous solutions mainly, where chemisorptions occur involving valency forces through sharing or the exchange of electrons between

Table 3 Values of thermodynamic parameters for cyanotoxin adsorption onto PPy/Fe₃O₄

| Cyanobacterial toxins | Temperature (K) | ΔG° (kJ mol ⁻¹) | ΔH° (kJ mol ⁻¹) | ΔS° (kJ mol ⁻¹ K ⁻¹) | R^2 |
|-----------------------|-----------------|--|--|--|--------|
| MC-LA | 293 | -9.987 | 136.34 | 0.496 | 0.9973 |
| | 303 | -13.603 | | | |
| | 313 | -22.900 | | | |
| | 323 | -28.465 | | | |
| MC-LR | 293 | -10.718 | 158.79 | 0.577 | 0.995 |
| | 303 | -17.13 | | | |
| | 313 | -26.283 | | | |
| | 323 | -33.03 | | | |
| MC-YR | 293 | -12.423 | 157.96 | 0.569 | 0.993 |
| | 303 | -19.145 | | | |
| | 313 | -29.145 | | | |
| | 323 | -34.373 | | | |
| MC-RR | 293 | -3.897 | 266.048 | 0.916 | 0.990 |
| | 303 | -10.58 | | | |
| | 313 | -23.94 | | | |
| | 323 | -33.299 | | | |
| CYN | 293 | -5.359 | 235.28 | 0.817 | 0.998 |
| | 303 | -12.091 | | | |
| | 313 | -28.364 | | | |
| | 323 | -35.716 | | | |

adsorbent and adsorbate (Ho 2006); in present study, the chloride ions of PPy were replaced by the negative charge carrying cyanotoxins. From Table 4, high-correlation values and proximity of data of adsorption capacities with experimental values reflected better fit for pseudo-second-order model in adsorption of cyanotoxins onto PPy/Fe₃O₄ from aqueous media.

Intraparticle diffusion model

The rate of adsorbate diffusion within the adsorbent pores controlled the process of intraparticle diffusion. The intraparticle diffusion changes with square root of time given by Weber and Morris (1963) as Eq. (7)

$$q_t = k_{id}t^{1/2} + C \quad (7)$$

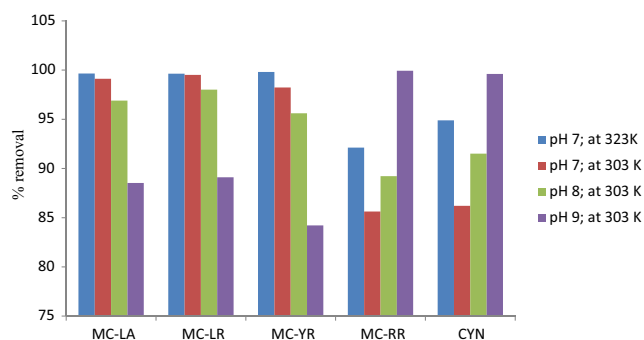


Fig. 6 Comparisons of cyanotoxins removal at 303 and 323 K at different pH

q_t ($\mu\text{g}/\text{mg}$) is the adsorbed amount onto the PPy/Fe₃O₄ at a time t (min), whereas k_{id} ($\mu\text{g}/\text{mg min}^{0.5}$) is the rate constant of intraparticle diffusion, which was evaluated from the slope of the linear plot of q_t versus $t^{1/2}$. If the regression of q_t versus $t^{1/2}$ is linear and passes through the origin, then intraparticle diffusion is the sole rate-limiting step. In present study, the regressions were linear for all the adsorbates and the plot did not pass through the origin (Fig. 7), thereby suggesting that intraparticle diffusions were related to the adsorption but not as a sole rate-controlling step. The rate constants of intraparticle diffusion at varying temperatures (303–323 K) are shown in Table 5. In order to understand the mechanism of adsorption of cyanotoxins onto PPy/Fe₃O₄, it has been divided into three stages. The first stage was called as an instantaneous adsorption, which happened because of electrostatic bond between cyanotoxins and the positive charged nitrogen (N^+) present on the surface of PPy/Fe₃O₄. The second stage was recognized as intraparticle diffusion of cyanotoxins within the PPy matrix through the pores present on the surface of conducting polymer which would have been formed during the processes of polymerization. The intraparticle diffusion process is considered as a gradual adsorption stage, since it might need adsorbates to change their molecular orientation depending upon the size of the pores, as discussed by Pendleton et al. (2001). The final stage corresponds to the equilibrium adsorption when adsorbates occupy all active or possible sites of the adsorbent. Among all the studied, cyanotoxin MC-RR, YR, and CYN have shown highest R^2 values at

Table 4 Adsorption kinetic model rate constant of PPy/Fe₃O₄ at different initial concentration of cyanotoxins

| Cyanotoxins | Initial concentration C ₀ (μg/L) | q _e (exp) (μg/mg) | Pseudo-first order | | | Pseudo-second order | | |
|-------------|--|------------------------------|------------------------------|--|----------------|---|------------------------------|----------------|
| | | | q _e (cal) (μg/mg) | k ₁ × 10 ⁻³ (min ⁻¹) | R ² | k ₂ × 10 ⁻³ (mg/μg min) | q _e (cal) (μg/mg) | R ² |
| MC-LA | 50 | 48.91 | 41.58 | 1.171 | 0.913 | 0.542 | 48.62 | 0.991 |
| | 100 | 68.15 | 58.75 | 0.842 | 0.924 | 0.032 | 67.74 | 0.994 |
| | 150 | 95.98 | 86.33 | 0.331 | 0.871 | 0.011 | 95.56 | 0.998 |
| MC-LR | 50 | 68.46 | 54.67 | 0.984 | 0.891 | 0.467 | 68.22 | 0.989 |
| | 100 | 91.51 | 72.25 | 0.801 | 0.851 | 0.041 | 91.43 | 0.990 |
| | 150 | 105.72 | 90.23 | 0.298 | 0.810 | 0.024 | 105.65 | 0.997 |
| MC-YR | 50 | 62.01 | 48.98 | 0.997 | 0.802 | 0.331 | 61.66 | 0.996 |
| | 100 | 73.32 | 66.53 | 0.854 | 0.899 | 0.061 | 72.98 | 0.992 |
| | 150 | 98.27 | 85.03 | 0.451 | 0.897 | 0.019 | 98.15 | 0.991 |
| MC-RR | 50 | 58.41 | 35.15 | 0.885 | 0.917 | 0.071 | 58.17 | 0.990 |
| | 100 | 62.34 | 54.85 | 0.613 | 0.931 | 0.037 | 62.23 | 0.995 |
| | 150 | 85.11 | 73.90 | 0.255 | 0.901 | 0.009 | 84.91 | 0.994 |
| CYN | 50 | 52.89 | 40.57 | 0.879 | 0.935 | 0.112 | 52.64 | 0.998 |
| | 100 | 79.63 | 61.62 | 0.542 | 0.934 | 0.015 | 79.39 | 0.995 |
| | 150 | 93.87 | 81.02 | 0.311 | 0.942 | 0.005 | 93.65 | 0.996 |

Fig. 7 Intraparticle diffusion plot of cyanotoxins at different temperature

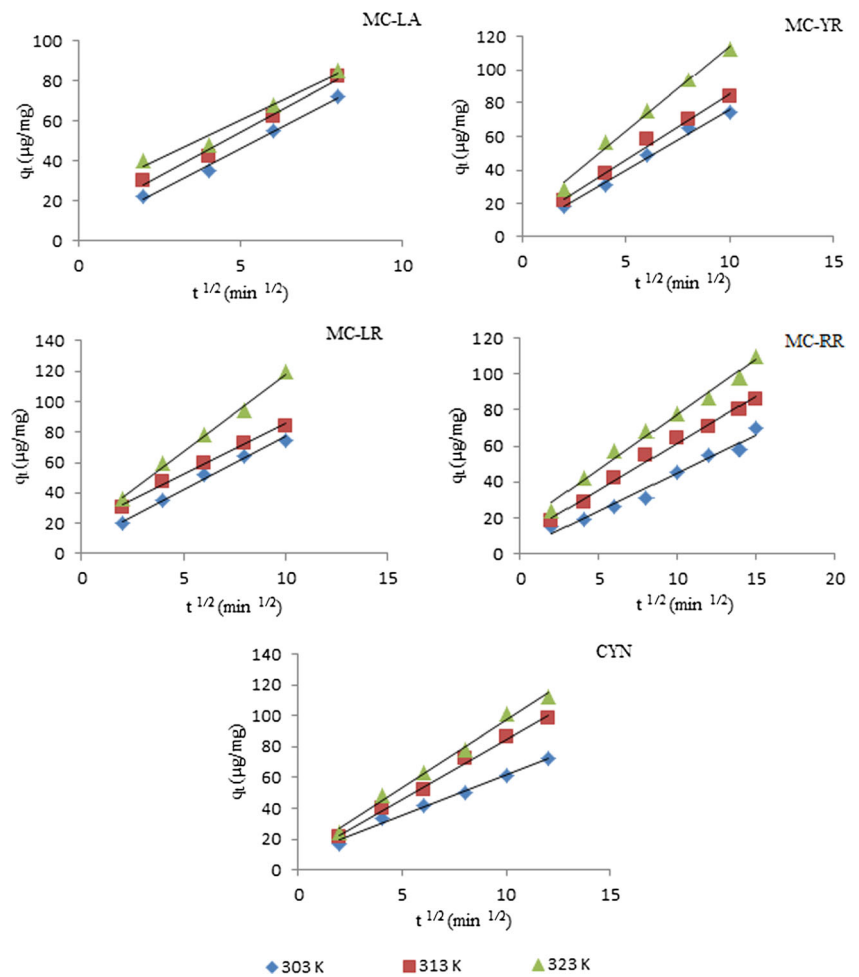


Table 5 Intraparticle rate parameter of cyanotoxins at different temperatures

| Cyanotoxins | Temperature (K) | k_{id} ($\mu\text{g}/\text{mg min}^{1/2}$) | C | R^2 |
|-------------|-----------------|--|-------|--------|
| MC-LA | 303 | 8.50 | 3.50 | 0.9938 |
| | 313 | 8.80 | 10.0 | 0.9878 |
| | 323 | 7.75 | 21.5 | 0.9744 |
| MC-LR | 303 | 6.95 | 7.5 | 0.9924 |
| | 313 | 6.70 | 18.6 | 0.9938 |
| | 323 | 10.10 | 17.0 | 0.9935 |
| MC-YR | 303 | 7.20 | 4.40 | 0.9897 |
| | 313 | 7.80 | 7.60 | 0.9928 |
| | 323 | 10.15 | 12.5 | 0.9913 |
| MC-RR | 303 | 4.20 | 2.57 | 0.9711 |
| | 313 | 5.14 | 9.97 | 0.9912 |
| | 323 | 6.08 | 16.49 | 0.9875 |
| CYN | 303 | 5.24 | 9.1 | 0.9904 |
| | 313 | 7.75 | 7.2 | 0.9945 |
| | 323 | 8.77 | 9.6 | 0.9915 |

temperature 313 K, which demonstrated that high temperature favors intraparticle diffusion in PPy/Fe₃O₄ adsorbent.

Table 6 Adsorption isotherms of PPy/Fe₃O₄ at different temperatures

| Cyanobacterial toxins | Temperature (K) | Langmuir constants | | | Freundlich constants | | | Sips constants | | | |
|-----------------------|-----------------|-----------------------------------|-------------------------|--------|-----------------------------------|-------|--------|-----------------------------------|-------------------------|-------|--------|
| | | Q^0 ($\mu\text{g}/\text{mg}$) | b (L/ μg) | R^2 | K_f ($\mu\text{g}/\text{mg}$) | b_f | R^2 | Q^0 ($\mu\text{g}/\text{mg}$) | b (L/ μg) | n | R^2 |
| MC-LA | 303 | 259.02 | 0.198 | 0.9998 | 27.92 | 0.083 | 0.9795 | 248.32 | 0.211 | 0.122 | 0.9891 |
| | 313 | 264.32 | 0.213 | 0.9996 | 31.51 | 0.147 | 0.9812 | 255.35 | 0.221 | 0.256 | 0.9878 |
| | 323 | 276.41 | 0.367 | 0.9990 | 34.34 | 0.165 | 0.9561 | 263.88 | 0.372 | 0.299 | 0.9811 |
| MC-LR | 303 | 301.11 | 0.178 | 0.9999 | 33.67 | 0.056 | 0.9305 | 291.09 | 0.197 | 0.098 | 0.9745 |
| | 313 | 314.04 | 0.196 | 0.9994 | 38.45 | 0.098 | 0.9762 | 299.67 | 0.213 | 0.123 | 0.9888 |
| | 323 | 321.19 | 0.298 | 0.9991 | 41.29 | 0.129 | 0.9856 | 303.45 | 0.310 | 0.134 | 0.9732 |
| MC-YR | 303 | 336.08 | 0.221 | 0.9998 | 18.94 | 0.094 | 0.9548 | 314.44 | 0.229 | 0.137 | 0.9645 |
| | 313 | 348.11 | 0.257 | 0.9990 | 22.07 | 0.115 | 0.9365 | 321.89 | 0.259 | 0.176 | 0.9696 |
| | 323 | 354.04 | 0.314 | 0.9992 | 27.32 | 0.186 | 0.8976 | 341.21 | 0.323 | 0.211 | 0.9112 |
| MC-RR | 303 | 238.91 | 0.216 | 0.9999 | 16.62 | 0.121 | 0.9657 | 221.24 | 0.229 | 0.198 | 0.9778 |
| | 313 | 337.38 | 0.231 | 0.9997 | 21.89 | 0.163 | 0.9143 | 298.78 | 0.237 | 0.212 | 0.9376 |
| | 323 | 360.14 | 0.334 | 0.9991 | 38.65 | 0.194 | 0.8897 | 349.65 | 0.345 | 0.226 | 0.9178 |
| CYN | 303 | 272.86 | 0.221 | 0.9999 | 19.90 | 0.119 | 0.9542 | 266.56 | 0.272 | 0.138 | 0.9765 |
| | 313 | 311.96 | 0.254 | 0.9993 | 21.54 | 0.148 | 0.9231 | 289.98 | 0.284 | 0.179 | 0.9367 |
| | 323 | 346.17 | 0.331 | 0.9990 | 24.47 | 0.176 | 0.8786 | 324.54 | 0.391 | 0.215 | 0.9019 |
| MC-RR ^a | 303 | 212.34 | 0.204 | 0.9999 | 15.32 | 0.113 | 0.9723 | 202.14 | 0.223 | 0.134 | 0.9799 |
| | 313 | 318.71 | 0.219 | 0.9992 | 20.14 | 0.142 | 0.9512 | 274.53 | 0.227 | 0.165 | 0.9676 |
| | 323 | 342.02 | 0.297 | 0.9994 | 36.67 | 0.169 | 0.8999 | 329.34 | 0.314 | 0.199 | 0.9122 |
| CYN ^a | 303 | 251.63 | 0.212 | 0.9996 | 16.98 | 0.101 | 0.9613 | 243.76 | 0.225 | 0.126 | 0.9667 |
| | 313 | 295.77 | 0.243 | 0.9993 | 18.18 | 0.127 | 0.9329 | 270.66 | 0.298 | 0.180 | 0.9656 |
| | 323 | 329.85 | 0.325 | 0.9990 | 21.72 | 0.149 | 0.9091 | 311.87 | 0.353 | 0.210 | 0.9376 |

^a Analysis at pH 7

Adsorption isotherms

To quantify the adsorption capacity of PPy/Fe₃O₄ for the removal of cyanotoxins from drinking water, the Langmuir and Freundlich isotherm models were used at various temperatures from 303 to 323 K. The cyanotoxins MC-LA, LR, and YR were analyzed at pH 7, while MC-RR and CYN at pH 9; however, MC-RR and CYN were analyzed at pH 7 also as for comparison since the prime aim of this study was to remove cyanotoxins from drinking water without alteration in pH.

Langmuir model

The data of the equilibrium studies for adsorption of cyanotoxins onto PPy/Fe₃O₄ particles follow the following form of Langmuir model (Eq. (8)).

$$C_e/Q_e = 1/Q^0b + C_e/Q^0 \tag{8}$$

where C_e was the equilibrium concentration ($\mu\text{g}/\text{L}$) of cyanotoxin in water and Q_e ($\mu\text{g}/\text{mg}$) was the amount adsorbed onto the surface of adsorbent at equilibrium. The value of b (L/ μg) relates the heat of adsorption, while the Langmuir constants Q^0 ($\mu\text{g}/\text{mg}$) represent the adsorption capacity of

monolayer adsorbent. The isotherm data Q^0 and b were calculated and reported in Table 6. It was observed that the uptake of cyanotoxins increased onto PPy/Fe₃O₄ with rise in temperature. High temperature increases the thermal energy of the adsorbing species which favors to higher adsorption capacity. However, the increases in Q^0 with increase in temperature were highest for MC-RR and CYN, in comparison to m-YR, LR, and LA, because heat required displacing the solvent (aqueous) are higher since they are less hydrophobic (Table 2). The high values of R^2 (0.9991–0.9999) shown in Table 6 advocate better a concurrence between the parameters of adsorption isotherm and confirmed the energetically equivalent units of monolayer adsorption of cyanotoxins onto Fe₃O₄ coated with polypyrrole surface.

Freundlich model

Freundlich model hints towards the conclusion that the adsorbent deals with the multilayer adsorption process due to the presence of energetically heterogeneous adsorption sites which is shown in linear form as in Eq. (9).

$$\ln Q_e = \ln K_f + b_f \ln C_e \tag{9}$$

where C_e is the equilibrium concentration of cyanotoxins in water sample (μg/L) and the amount of toxins adsorbed on the matrix of conducting polymer (μg/mg), K_f is the Freundlich equilibrium constant, and b_f is an experimental parameter which describe the intensity of adsorption related with heterogeneity of the adsorbent surface. The adsorption is considered as favorable if the value of b_f lies in between 0.1 and 1. The related experimental parameters were determined and listed in Table 6. The closer the values of b_f towards 1, the better the favorability of adsorption is.

Sips model

The Sips model is combination of the Langmuir and Freundlich isotherm models that can be used to represent equilibrium adsorption data. The Sips model takes the following form for representing adsorbate equilibrium data as shown in Eq. (10):

$$Q_e = Q^0 b C_e^{1/n} / 1 + b C_e^{1/n} \tag{10}$$

where C_e (μg/L) is the equilibrium concentration of cyanotoxins in water sample and Q_e (μg/mg) is the amount of toxins adsorbed on the matrix of conducting polymer, where Q^0 (μg/mg) and n are the Sips constant characteristics of the system, indicating the maximum cyanotoxin uptake and adsorption intensity, respectively. The Sips model provided slightly lower values of Q^0 for all the cyanotoxins studied than those obtained with the Langmuir model. However, the value of R^2 in Sips model that varies in between 0.9891 and 0.9019

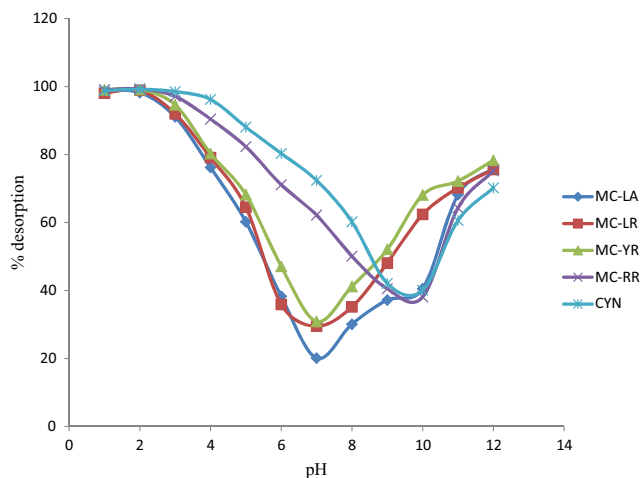


Fig. 8 Effect of pH on desorption of cyanotoxins from PPy/Fe₃O₄ nanoparticles

as shown in Table 6 indicates inferior accord between the parameters of adsorption isotherm, comparing to Langmuir model.

In Table 6, the data revealed that the Langmuir adsorption isotherm model yielded the best fit as indicated by the highest R^2 values compared to the other models for all cyanotoxins, showing that the adsorptions of them onto the PPy surface were homogeneous and monolayer in nature. Previous researches (Pendleton et al. 2001; Sathishkumar et al. 2010) also reported that Langmuir isotherm model is suitable for cyanotoxin evaluation.

From Table 6, it was evident that the Langmuir monolayer adsorption capacity increased by 6.71, 6.66, 5.33, 50.74, and 26.86 %, for MC-LA, LR, YR, RR, and CYN, respectively, with an increase in temperature from 303 to 323 K. The effects of temperature changes were highest in case of MC-RR and followed by CYN, while MC-LA, LR, and YR showed almost equal and low percent of increase in adsorption capacity. The Sips model produced the second best fitting isotherm parameter values for all the cases studied and low error values. The magnitude of b that increased with temperature confirmed the

Table 7 Adsorption capacity of PPy/Fe₃O₄ at 303 K

| Cycles | Adsorption capacity (μg/mg) | | | | |
|--------|-----------------------------|--------|--------|--------|--------|
| | MC-LA | MC-LR | MC-YR | MC-RR | CYN |
| I | 259.02 | 301.11 | 336.08 | 238.91 | 272.86 |
| II | 256.17 | 298.05 | 332.97 | 236.74 | 270.67 |
| III | 252.54 | 294.48 | 329.36 | 234.37 | 267.94 |
| IV | 247.36 | 288.46 | 323.30 | 230.29 | 263.58 |
| V | 235.96 | 276.41 | 311.21 | 222.17 | 254.85 |
| VI | 216.90 | 251.40 | 288.02 | 208.08 | 238.75 |
| VII | 191.59 | 225.31 | 255.77 | 185.38 | 212.56 |
| VIII | 156.60 | 189.09 | 231.92 | 165.32 | 190.42 |

Table 8 Comparison of adsorption capacities of cyanotoxins with other adsorbents

| Adsorbents | Cyanotoxins | Adsorption capacity | Contact time | pH | Model | Reference |
|--|-------------|-------------------------|--------------|-------|------------|--------------------------|
| Darco, G-60, wood PAC | MC-LR | 1259 $\mu\text{g/g}$ | 7 days | 8.5 | Freundlich | Mohamed et al. 1999 |
| Pine wood activated carbon | MC-LR | 200 $\mu\text{g/mg}$ | 10 min | 6–8.5 | Langmuir | Júnior et al. 2008 |
| Sugar cane bagasse activated carbon | MC-LR | 161 $\mu\text{g/mg}$ | 10 min | 6–8.5 | Langmuir | Junior et al. 2008 |
| Wood-based activated carbon | MC-LR | 196 $\mu\text{g/mg}$ | 72 h | 2.5 | Langmuir | Pendleton et al. 2001 |
| Coconut shell activated carbon G1 | MC-LR | 16.1 mg/g | 24 h | 7.5 | Langmuir | Huang et al. 2007 |
| Wood-based activated carbon G3 | MC-LR | 83.3 mg/g | 24 h | 7.5 | Langmuir | Huang et al. 2007 |
| Wood activated carbon | MC-LR | 220 $\mu\text{g/mg}$ | – | – | Langmuir | Donati et al. 1994 |
| Peat | MC-LR | 286 $\mu\text{g/g}$ | 30 min | 3.0 | Langmuir | Sathishkumar et al. 2010 |
| Pumice | MC-LR | 21.5 $\mu\text{g/g}$ | – | 4.0 | – | Gurbuz and Codd 2008 |
| Waste rubber wood activated carbon | MC-LR | 296.57 $\mu\text{g/mg}$ | 300 min | 7.0 | Langmuir | Hena et al. 2014 |
| Carbon nanotubes | MC-RR | 14.8 mg/g | 8 h | 7.0 | – | Yan et al. 2006 |
| Carbon nanotubes | MC-LR | 5.9 mg/g | 8 h | 7.0 | – | Yan et al. 2006 |
| Graphene oxide | MC-RR | 1877.8 $\mu\text{g/g}$ | 5 min | 5.0 | Langmuir | Pavagadhi et al. 2013 |
| Graphene oxide | MC-LR | 1699.7 $\mu\text{g/g}$ | 5 min | 5.0 | Langmuir | Pavagadhi et al. 2013 |
| Coal-based steam-activated powdered carbon | CYN | 0.17 mg/g | 3 days | 7.9 | Freundlich | Ho et al. 2008 |
| Chemically activated powdered carbon | CYN | 0.13 mg/g | 3 days | 7.9 | Freundlich | Ho et al. 2008 |
| Chemically activated powdered carbon | MC-LR | 1.14 mg/g | 60 min | 7–8 | Freundlich | Cook and Newcombe 2008 |
| Wood-based, chemically activated powdered carbon | MC-LA | 0.412 mg/g | 60 min | 7–8 | Freundlich | Cook and Newcombe 2008 |
| Magnetic mesoporous silica microsphere | MC-LR | 160 $\mu\text{g/mg}$ | 5 min | 7.0 | – | Deng et al. 2008 |
| Magnetic mesoporous silica microsphere | MC-RR | 140 $\mu\text{g/mg}$ | 5 min | 7.0 | – | Deng et al. 2008 |
| Magnetic mesoporous silica microsphere | MC-YR | 160 $\mu\text{g/mg}$ | 5 min | 7.0 | – | Deng et al. 2008 |
| PPy/Fe ₃ O ₄ | MC-LA | 259.02 $\mu\text{g/mg}$ | 8 min | 7.0 | Langmuir | Present study |
| PPy/Fe ₃ O ₄ | MC-LR | 301.11 $\mu\text{g/mg}$ | 10 min | 7.0 | Langmuir | Present study |
| PPy/Fe ₃ O ₄ | MC-YR | 336.08 $\mu\text{g/mg}$ | 10 min | 7.0 | Langmuir | Present study |
| PPy/Fe ₃ O ₄ | MC-RR | 238.91 $\mu\text{g/mg}$ | 15 min | 9.0 | Langmuir | Present study |
| PPy/Fe ₃ O ₄ | CYN | 272.86 $\mu\text{g/mg}$ | 12 min | 9.0 | Langmuir | Present study |

endothermic nature of adsorption, while increase in Freundlich constant b_f with temperature shows the favorability of cyanotoxin adsorption onto PPy surface at higher temperatures. Nevertheless, the comparative studies of adsorption isotherms for MC-RR and CYN confirmed that the adsorption capacities decreased at pH 7 comparing with the values obtained at pH 9 almost by 11 and 7.8 % at 303 K, 5.5 and 5.2 % at 313 K, and 5 and 4.7 % at 323 K, respectively.

Possible adsorption mechanism

Below pH 10.5, the zeta potentials of PPy/Fe₃O₄ were positive, and over the range of pH 4 to 10, it remained relatively constant (approximately 37.4 mV). All targeted cyanotoxins possessed net negative charge except MC-RR and CYN up to pH 8.5, whereas MC-RR and CYN possessed negative charge at and above pH 9. At pH 7, the positive sites on PPy surface and net negative charges of MC-LA, LR, and YR and their

high hydrophobicity favor strong electrostatic attraction between adsorbent and adsorbates, without any alteration in quality of drinking water. However, comparatively low hydrophobicity of MC-RR and CYN have shown better adsorption at higher temperature; this might had happen due to the utilization of heat energy in displacement of solvent molecules (Pendleton et al. 2001). Thus, it can be concluded that adsorption of cyanotoxins onto Fe₃O₄-coated PPy layer govern by two major factors: (i) electrostatic force of attraction between pair ions and (ii) solubility of adsorbates. Highly soluble adsorbate showed less adsorption onto adsorbent, which can be increased by increase in temperature, since high temperature favors adsorption as well as intraparticle diffusion.

Desorption studies

The ability of regeneration of used PPy/Fe₃O₄ nanoparticle material after removal of cyanotoxins is an important factor

to evaluate the cost-effectiveness and environmental friendliness of an adsorbent. The results of cyanotoxin desorption from PPy/Fe₃O₄ nanoparticle are compiled in Fig. 8; shown pH 2 is the best condition to desorb almost 99 % of all the adsorbed cyanotoxins. Since the percent desorption at pH 1 was same as pH 2, thus to avoid the extreme condition, pH 2 was selected as the most favorable pH for desorption process. The percent desorption decreased with the increase of pH for MC-LR, LA, and YR and reached to their least desorption values at pH 7, which again start to increase with increase of pH. Up to pH 3, MC-LR, LA, and YR show net positive charge which obviously caused repulsion with dominantly positively charged adsorbent and lead to desorption. Minimum desorption occurred in between pH 6 and 8, where MC-LR, LA, and YR showed dominantly net negative charges. The same trend has been reported with MC-RR and CYN, where these two cyanotoxins reached to their least desorption values at pH 10, which again started to increase with increase of pH. Increments in percent desorption of cyanotoxins MC-RR and CYN had happened because of acquiring negative zeta potential on PPy particles above pH 10.8. The adsorption capacities of PPy/Fe₃O₄ nanoparticles decreased from 6.6 to 8.9 % depending upon cyanotoxins, after using five times as shown in Table 7. Reductions in adsorption capacities were reported as 30–40 % after using the same PPy/Fe₃O₄ nanoparticles for eight times. Even after using it for eight times, the adsorption capacities were found better than many reported adsorbent as listed in Table 8. Therefore, the proposed adsorbent can be successfully reused for multiple adsorption-desorption cycles with gradual loss of its original adsorption capacity. The quality of PPy/Fe₃O₄ nanoparticles deteriorated or efficiency of adsorbent decreased little faster with MC-LA, representing almost 40 % loss in efficiency after eight cycles. The efficiency losses of PPy/Fe₃O₄ nanoparticles were in the sequence of MC-LA > LR > YR > RR ≈ CYN.

Comparison of Fe₃O₄-coated PPy with other adsorbents

In order to prove the superiority of the proposed adsorbent over others, the comparison has been done as shown in Table 8, on the basis of adsorption capacity, time required to achieve equilibrium, and alteration in quality of water. It can be observed that at low pH, the adsorptions of cyanotoxins were high regardless the type of toxins and adsorbents. This is accepted with the fact that most of the adsorbents used for the removal of cyanotoxins were activated carbons from different origin. However, the activated carbons are good adsorbents for the removal of cyanotoxins since they contain negative charges, and to exploit the maximum advantages of activated carbon for removal of cyanotoxins, the pH of the water had been kept as acidic to acquire positive net charge on cyanotoxins. This leads to compromise the quality of drinking

water and added extra cost to neutralize it before supply. It was also noticed that generally, removal at neutral pH or close range of neutral pH, either the time of adsorption equilibrium were high (300 min to 7 days) or the adsorption capacities were low. However, here, the proposed adsorbent Fe₃O₄ coated with polypyrrole was found to have a relatively large adsorption capacity, which proved to be a promising material for the removal of cyanotoxins from drinking water safely without altering the pH of water.

Conclusion

Magnetic nanoparticle coated with electro-conducting polypyrrole comprises a remarkable potentiality to remove cyanotoxins from water. PPy/Fe₃O₄ nanoparticle provides a cost-effective and environmental friendly process for removal of cyanotoxins. High adsorption capacity and short time requirement for equilibrium establishment are significant advantages of PPy/Fe₃O₄ nanoparticle over many other frequently used adsorbents. The cyanotoxin adsorption equilibrium data fitted very well to Langmuir adsorption isotherm model, and the mechanism was considered to be mainly due to the electrostatic attraction between the nanoparticles and cyanotoxins. The adsorption capacities that increased with rise in temperature revealed that the adsorptions were endothermic, which were also confirmed by the evaluated thermodynamic parameters. The ability of regeneration of PPy/Fe₃O₄ nanoparticle material after removal of cyanotoxins confirmed the reusability of the nanoparticles for next cycle of cyanotoxin adsorption.

Acknowledgment This research was financially supported by Malaysian Department of Higher Education through disbursement of Fundamental Research Grant Scheme 203/PTEKIND/6711465.

References

- Ansari R, Fahim NK (2007) Application of polypyrrole coated on wood sawdust for removal of Cr(VI) ion from aqueous solutions. *React Funct Polym* 67:367–374
- Ansari R, Fahim NK, Dellavar AF (2009) Removal of thiocyanate ions from aqueous solutions using polypyrrole and polyaniline conducting electroactive polymers. *J Iran Chem Res* 2:163–171
- Bhaumik M, Maity A, Srinivasu VV, Onyango MS (2011a) Enhanced removal of Cr(VI) from aqueous solution using polypyrrole/Fe₃O₄ magnetic nanocomposite. *J Hazard Mater* 190:381–390
- Bhaumik M, Leswif TY, Maity A, Srinivasu VV, Onyango MS (2011b) Removal of fluoride from aqueous solution by polypyrrole/Fe₃O₄ magnetic nanocomposite. *J Hazard Mater* 186:150–159
- Cook D, Newcombe G (2008) Comparison and modeling of the adsorption of two microcystin analogues onto powdered activated carbon. *Environ Technol* 29:525–534

- de Albuquerque Júnior EC, Méndez MOA, dos Reis Coutinho A, Franco TT (2008) Removal of cyanobacteria toxins from drinking water by adsorption on activated carbon fibers. *Mater Res* 11:371–380
- Deng Y, Qi D, Deng C, Zhang X, Zhao D (2008) Superparamagnetic high-magnetization microspheres with an Fe₃O₄@SiO₂ core and perpendicularly aligned mesoporous SiO₂ shell for removal of microcystins. *J Am Chem Soc* 130:28–29
- Dixon MB, Falconet C, Ho L, Chow CWK, O'Neill BK, Newcombe G (2010) Nanofiltration for the removal of algal metabolites and the effects of fouling. *Water Sci Technol* 61:1189–1199
- Dixon MB, Falconet C, Ho L, Chow CWK, O'Neill BK, Newcombe G (2011) Removal of cyanobacterial metabolites by nanofiltration from two treated waters. *J Hazard Mater* 188:288–295
- Donati C, Drikas M, Hayes R, Newcombe G (1994) Microcystin-LR adsorption by powdered activated carbon. *Water Res* 28:1735–1742
- Dunlop DJ, Ozdemir O (1997) *Rock magnetism: fundamentals and frontiers*. Cambridge University Press, Cambridge
- Eisazadeh H (2008) Removal of arsenic in water using polypyrrole and its composites. *World Appl Sci J* 3:10–13
- El-Sheikh SM, Zhang G, El-Hosainy HM, Ismail AA, O'Shea KE, Falaras P, Kontos AG, Dionysiou DD (2014) High performance sulfur, nitrogen and carbon doped mesoporous anatase-brookite TiO₂ photocatalyst for the removal of microcystin-LR under visible light irradiation. *J Hazard Mater* 280:723–733
- Falconer IR (1989) Effects on human health of some toxic cyanobacteria (blue-green algae) in reservoirs, lakes, and rivers. *Toxicity Assess* 4:175–184
- Falconer IR (2005) *Cyanobacterial toxins of drinking water supplies: cylindrospermopsins and microcystins*. CRC Press, Boca Raton
- Fotiou T, Triantis T, Kaloudis T, Hiskia A (2015) Photocatalytic degradation of cylindrospermopsin under UV-A, solar and visible light using TiO₂. Mineralization and intermediate products. *Chemosphere* 119:S89–S94
- Gurbuz F, Codd GA (2008) Microcystin removal by a naturally-occurring substance: pumice. *Bull Environ Contam Toxicol* 81:323–327
- He X, de la Cruz AA, O'Shea KE, Dionysiou DD (2014) Kinetics and mechanisms of cylindrospermopsin destruction by sulfate radical-based advanced oxidation processes. *Water Res* 63:168–178
- Hena S (2010) Removal of chromium hexavalent ion from aqueous solutions using biopolymer chitosan coated with poly 3-methyl thiophene polymer. *J Hazard Mater* 181:474–479
- Hena S, Ismail N, Isaam AM, Ahmad A, Bhawani SA (2014) Removal of microcystin-LR from aqueous solutions using % burn-off activated carbon of waste wood material. *J Water Supply Res Technol AQUA* 63:332–341
- Ho YS (2006) Review of second-order models for adsorption systems. *J Hazard Mater* 136:681–689
- Ho L, Slyman N, Kaeding U, Newcombe G (2008) Optimizing PAC and chlorination practices for cylindrospermopsin removal. *J Am Water Works Assoc* 100:88–96
- Ho L, Lambling P, Bustamante H, Duker P, Newcombe G (2011) Application of powdered activated carbon for the adsorption of cylindrospermopsin and microcystin toxins from drinking water supplies. *Water Res* 45:2954–2964
- Huang WJ, Cheng BL, Cheng YL (2007) Adsorption of microcystin-LR by three types of activated carbon. *J Hazard Mater* 141:115–122
- Jones GJ, Orr PT (1994) Release and degradation of microcystin following algicide treatment of a *Microcystis aeruginosa* bloom in a recreational lake, as determined by HPLC and protein phosphatase inhibition assay. *Water Res* 28:871–876
- Lagergren S (1898) About the theory of so called adsorption of soluble substances, *Kungliga Svenska Vetenskapsakademiens. Handlingar Band 24(04):1–39*
- Mohamed ZA, Carmichael WW, El-Sharouny J, An HM (1999) Activated carbon: removal efficiency of microcystins in an aqueous cell extract of *Microcystis aeruginosa* and *Oscillatoria tenuis* strains isolated from Egyptian freshwaters. *Environ Toxicol* 14:197–201
- Pavagadhi S, Tang ALL, Sathishkumar M, Loh KP, Balasubramanian R (2013) Removal of microcystin-LR and microcystin-RR by graphene oxide: adsorption and kinetic experiments. *Water Res* 47:4621–4629
- Pearl HW, Huisman J (2008) Climate: blooms like it hot. *Science* 320:57–58
- Pendleton P, Schumann R, Wong SH (2001) Microcystin-LR adsorption by activated carbon. *J Colloid Interface Sci* 240:1–8
- Sathishkumar M, Binupriya AR, Swaminathan K, Choi JG, Yun SE (2008) Arsenite sorption in liquid phase by *Aspergillus fumigatus*: adsorption rates and isotherm studies. *J Microbiol Biotechnol* 24:1813–1820
- Sathishkumar M, Pavagadhi S, Mahadevan A, Balasubramanian R (2010) Removal of a potent cyanobacterial hepatotoxin by peat. *J Environ Sci Health, Part A: Tox Hazard Subst Environ Eng* 45:1877–1884
- Wang H, Ho L, Lewis DM, Brookes JD, Newcombe G (2007) Discriminating and assessing adsorption and biodegradation removal mechanisms during granular activated carbon filtration of microcystin toxins. *Water Res* 41:4262–4270
- Wang F, Wu Y, Gao Y, Chen Z (2014) Biodegradation of microcystin-LR by *Burkholderia vietnamiensis*. *Chin J Environ Eng* 8:3837–3842
- Weber WJ, Morris JC (1963) Kinetics of adsorption on carbon from solution. *J Sanit Eng Div Am Soc Civ Eng* 89:31–60
- Yan H, Gong A, He H, Zhou J, Wei Y, Lv L (2006) Adsorption of microcystins by carbon nanotubes. *Chemosphere* 62:42–148
- Zhang X, Bai R (2003) Surface electric properties of polypyrrole in aqueous solutions. *Langmuir* 19:10703–10709
- Zhang G, Zhang YC, Nadagouda M, Han C, O'Shea K, El-Sheikh SM, Ismail AA, Dionysiou DD (2014) Visible light-sensitized S, N and C co-doped polymorphic TiO₂ for photocatalytic destruction of microcystin-LR. *Appl Catal B Environ* 144:614–621